
Homomorphism Autoencoder — Learning Group Structured Representations from Observed Transitions

Hamza Keurti^{1,2,3} Hsiao-Ru Pan¹ Michel Besserve¹
Benjamin F. Grewe² Bernhard Schölkopf¹

¹Max Planck Institute for Intelligent Systems, Tübingen, Germany

²Institute of Neuroinformatics, ETH Zürich, Switzerland

³Max Planck ETH Center for Learning Systems

{hamza.keurti,hpan,michel.besserve,bs}@tuebingen.mpg.de
bgrewe@ethz.ch

Abstract

How can we acquire world models that veridically represent the outside world both in terms of what is there and in terms of how our actions affect it? Can we acquire such models by interacting with the world, and can we state mathematical desiderata for their relationship with a hypothetical reality existing outside our heads? As machine learning is moving towards representations containing not just observational but also interventional knowledge, we study these problems using tools from representation learning and group theory. Under the assumption that our actuators act upon the world, we propose methods to learn internal representations of not just sensory information but also of actions that modify our sensory representations in a way that is consistent with the actions and transitions in the world. We use an autoencoder equipped with a group representation linearly acting on its latent space, trained on 2-step reconstruction such as to enforce a suitable homomorphism property on the group representation. Compared to existing work, our approach makes fewer assumptions on the group representation and on which transformations the agent can sample from the group. We motivate our method theoretically, and demonstrate empirically that it can learn the correct representation of the groups and the topology of the environment. We also compare its performance in trajectory prediction with previous methods.

1 Introduction

One of the most enigmatic questions addressed by mammalian intelligence is how to build a simple internal model of the external world that represents all behavior-relevant information. Humans seem to acquire such internal models by interacting with the world, but it is unclear what type of structure is embedded internally and how this can be realized in machine learning (ML). As ML is moving towards representations that carry more than just observational information [Sutton and Barto, 2015, Schölkopf et al., 2021], we assay whether current tools may allow us to study the above question from the point of view of ML, adding to the recent interest in interactive and geometric structure learning [Cohen and Welling, 2016, Eslami et al., 2018].

Taking inspiration from neuroscience, we point out that when, for example, animals use their motor apparatus to act, efference copies of motor signals in the form of neuronal activities are directly sent to the brain’s sensory system. Subsequently, these motor signals are integrated with incoming sensory observations to predict future sensory inputs [Keller et al., 2012]. Here, we argue that such efference copies can be useful for learning structured latent representations of sensory observations and for

disentangling the key latent factors of behavior relevance. This view is also in line with hypotheses formulated by developmental psychology [Piaget, 1964], stating that perceiving an object is not creating a mental copy of it but rather internalizing an understanding of how this object transforms under different interventions. For our approach, we translate this idea into an artificial setting in which an agent has to build an internal representation of its environment through interacting and observing. To modify its environment, the agent is allowed to perform a simple set of transformations while observing the impact of its actions. In artificial intelligence, this type of interactive learning has recently sparked interest for many lines of research that develop new algorithms to allow agents to discover their sensorimotor cascades [Censi and Murray, 2012].

In our specific case, the agent’s actions organize, at least locally, in a group so that actions can be composed. In particular, the agent can perform the identity action of doing nothing and the inverse action to reverse the impact of a preceding action on the environment. Further, for learning the environmental transformations in response to its actions, the agent needs to learn a sensory latent space that is consistent with its observations. The learning of the action-observation relationship then amounts to predicting the change in the agent’s latent sensory space using the incoming motor commands [Chaudhuri et al., 2019]. Mathematically, this corresponds to an equivariance property of the sensory representations with regard to the group acting on the environment.

While one can mathematically create infinitely many of such representations, an agent with bounded computational abilities always needs to choose one allowing efficient manipulation, interpretation and prediction of changes in its environment. A representational property compatible with this desideratum is disentanglement [Bengio et al., 2012, Kulkarni et al., 2015] which states that the latent representation can be decomposed into (groups of) scalar latent variables reflecting interpretable properties of the environment that the agent can modify independently. A group theoretic account of representations has been proposed in Higgins et al. [2018], which defined disentanglement grounded in symmetries of the world. Caselles-Dupré et al. [2019] proved that such symmetry-based disentanglement requires interaction with the environment to observe the effect of symmetries. Following this principle, Quessard et al. [2020] investigated learning group structured representations from data. However, these studies assumed an already known group decomposition through only allowing the agent to perform actions sampled from the independent subgroups but not their composition.

In the present work, we investigate how a disentangled group structured representation can be learned based on observation-action sequences carried out by an agent embedded in an environment. Our approach only requires minimal prior assumptions with respect to the latent structure to be learned. In particular, instead of directly enforcing a parametrized representation of a particular group, we allow for arbitrary mappings to a subspace of linear maps. Our mapping is naturally shaped into a disentangled group representation by observing how actions and their successions transform the image space. We propose a training loss derived from the commutative diagram that an equivariant map satisfies. We implement a predictive autoencoder that we call homomorphism autoencoder (HAE) that is trained on an equivariance constraint and we show performance exceeding previous approaches while relying only on minimal priors about the group structure to be learned.

Our contributions can be summarized as follows:

- We propose the HAE framework to jointly learn a group representation of transitions, as well as a symmetry-based disentangled representation of observations with minimal assumptions on the group.
- We show theoretically and experimentally that the HAE learns the group structure of the set of transitions.
- In addition, when the group of symmetries the agent can sample from does not explain all variations in the observed stimuli, the HAE separates the acted-on factors (pose) from the non acted-on factors (identity).

Related Work. Learning useful representations has been approached with a wide range of methods. When learning from observational data only, generative models such as Variational Autoencoders often have difficulties to infer ground truth disentangled factors without additional assumptions on the ground truth mechanisms [Locatello et al., 2019]. On the one hand, in the i.i.d data setting, there are theoretical and empirical results supporting that constraining the function class that maps the true latent factors to the observations is beneficial to identifying these factors [Gresele et al., 2021]. In contrast, access to non-i.i.d data, e.g. from multiple environments, has been shown to allow to

uncover ground truth latent factors, notably through contrastive learning approaches [Hyvarinen and Morioka, 2016, Khemakhem et al., 2020, von Kügelgen et al., 2021]. This is also in line with methods relying on interventional data, which provides more information about representational structure. For instance, Sontakke et al. [2021] propose disentangling binary factors of variations by learning interactions which best separate sensory trajectories. Thomas et al. [2017] propose a specific objective function that leads agents to learn policies that separately act on the disentangled properties of the environment. The work closest to ours is that of Quessard et al. [2020], addressing learning from interactions but assuming an already known group decomposition, and learning exclusively through the observation of actions from individual subgroups but not their composition.

2 Background

2.1 Symmetry-Based Disentangled Representation Learning - SBDRL

Following the group theoretic formalism introduced by Higgins et al. [2018], we assume the set of observations $O \in R^{n_x \times n_y}$ is obtained from a set of world states W through an unseen *generative process* $b : W \rightarrow O$. An *inference process* $h : O \rightarrow Z$ maps observations to their vector representations.

A group of symmetries G structures the world states set by its action $\cdot_W : G \times W \rightarrow W$. G is decomposed into a direct product of subgroups $G = G_1 \times \dots \times G_n$. Here, each subgroup only transforms a specific latent property while keeping all others constant. (We refer to Appendix A for background on groups and group actions.)

A representation is a symmetry based representation if it verifies the commutative diagram in Figure 1. It then satisfies:

1. There is a (non-trivial) action of G on Z :

$$\cdot_Z : G \times Z \rightarrow Z.$$
2. The composition $f = h \circ b : W \rightarrow Z$ is equivariant, meaning that transformations of W are reflected on Z . Formally, f and the group action commute:

$$\forall g \in G, w \in W, \quad f(g \cdot_W w) = g \cdot_Z f(w).$$

The symmetry based representation is disentangled with regard to the group decomposition $G = G_1 \times \dots \times G_n$ if it satisfies this additional condition:

3. Z can be written as a product of spaces $Z = Z_1 \times \dots \times Z_n$ or as a direct sum of subspaces $Z = Z_1 \oplus \dots \oplus Z_n$ such that each subgroup G_i acts non trivially on Z_i and acts trivially on Z_j for $j \neq i$.

A group action $\cdot_Z : G \times Z \rightarrow Z$ induces a group homomorphism $\rho : G \rightarrow \text{Sym}(Z)$ where $\text{Sym}(Z)$ is the group of invertible mappings from Z to itself (more in Appendix A). If we require the group action \cdot_Z on Z to be linear, then the existence of a group action on Z is equivalent to the existence of a homomorphism $\rho : G \rightarrow \text{GL}(Z)$, called a group representation. The disentanglement condition is then expressed as follows:

3. (Linear) There exists a decomposition $Z = Z_1 \oplus \dots \oplus Z_n$ and a decomposition of the group representation $\rho = \rho_1 \oplus \dots \oplus \rho_n$ where each $\rho_i : G_i \rightarrow \text{GL}(Z_i)$ is a subrepresentation.

The action on Z can then be written

$$g \cdot_Z z = \rho(g_1, \dots, g_n)(z_1 \oplus \dots \oplus z_n) = \rho_1(g_1)z_1 \oplus \dots \oplus \rho_n(g_n)z_n, \quad (1)$$

for $g = (g_1, \dots, g_n) \in G$ and $z = z_1 \oplus \dots \oplus z_n \in Z$. Clearly each subgroup G_i acts trivially on Z_j , $j \neq i$.

We assume the agent generates all observations through interacting with its environment, thus the group elements are observed through its actions. Now the goal for the agent is to learn both the inference process h and a disentangled group representation ρ using the HAE, described in Subsection 3.2.

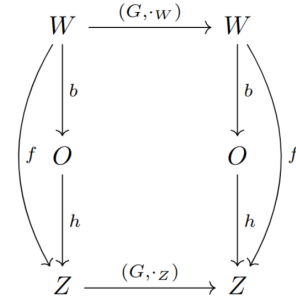


Figure 1: Commutative diagram for a symmetry based representation.

2.2 Observing Symmetries

Caselles-Dupré et al. [2019] proved that learning such symmetry-based disentangled representations requires observing the group elements that transition one state of the world into another (consequently one observation to the next). Similarly to past works [Quessard et al., 2020, Caselles-Dupré et al., 2019], we suggest using the interventions of an agent on its environment as a means to probe the symmetries of the environment. However, we do not assume that these interventions only act on one latent at a time.

Instead, the agent’s interventions could modify one or multiple latents without prior knowledge of which latents were modified. Furthermore, the intervention signals are obtained from a neighborhood of the group’s identity through an unknown deterministic mapping φ (that also carries the local group structure). These signals therefore do not parametrize explicitly the separate latents.

For a given group element, we denote \tilde{g} , its representation with regard to the true latents, for instance as detailed in Section 3.1, this could be the difference between latent vectors. And we denote g the representation with regard to the action performed by the agent. For a biological agent, g could be the efference copy, a copy of the motor neural signals sent to the brain to be processed together with sensory information. For a robotic agent, g could be a copy of the motor command.

We assume there exists a deterministic mapping between parametrizations $\varphi : \tilde{g} \mapsto g$. For instance, when a person moves a chalk along a blackboard, the chalk describes a 2D movement \tilde{g} , whereas the person’s movement is overparametrized by the rotation angles of the joints of the arm $g = \varphi(\tilde{g})$.

2.3 Lie Groups and the Exponential Map

When a group G is also a differentiable manifold it is called a Lie Group. The tangent space to the group G at the identity forms a Lie Algebra \mathfrak{g} : A vector space equipped with a bilinear product, the Lie bracket. We will leverage a convenient property of Lie Groups and their Lie Algebras that is the group can be studied through its tangent space. Indeed, the matrix exponential, called the exponential map in this setting, transports elements from the Lie Algebra to the Lie Group. Under certain assumptions, for instance if G is connected compact, the exponential map is surjective and therefore the whole group G can be described from the tangent space at its identity.

The exponential of an arbitrary matrix A is given by the series $e^A = \sum_{k=0}^{\infty} \frac{1}{k!} A^k$.

We assume the group of observed transitions G is a connected compact Lie Group. The exponential map is surjective on it and the group representation ρ can be obtained by composing the exponential map with a mapping ϕ to the Lie Algebra \mathfrak{g} . We use a neural network to learn the mapping ϕ .

$$\rho : G \xrightarrow{\phi} \mathfrak{g} \xrightarrow{\exp} GL(Z)$$

3 The HAE approach and experimental setup

3.1 Transition Dataset

To illustrate our approach, we consider the dSprites dataset [Matthey et al., 2017], a labelled image dataset of 2D shapes (square, heart and ellipse) varied in scale, orientation and x and y positions, all of these factors of variations can be seen as the vector of latents w . We modify the dataset to observe transitions $(o_1, \tilde{g}_1, o_2, \tilde{g}_2, \dots, \tilde{g}_{N-1}, o_N)$, where \tilde{g}_i ’s correspond to differences of the latent vectors w_{i+1} and w_i , they also parametrize the Lie Group of translations on the latents’ manifold. For most experiments, we limit ourselves to the cyclic translations of the x and y position, cyclic in the sense that the vertical boundaries of the image are glued together and the horizontal boundaries are glued together, as such making the set of (x, y) positions a torus.

3.2 The Homomorphism Autoencoder (HAE) architecture.

To jointly learn the latent representation h of the observations and the group representation ρ , we introduce the 2-step HAE, described in Figure 2, which is made up of an encoder network h , a decoder network d mirroring the architecture of h and a group representation ρ , which is the composition of a neural network ϕ and the matrix exponential. The group representation $\rho : G \rightarrow GL(Z)$ acts on

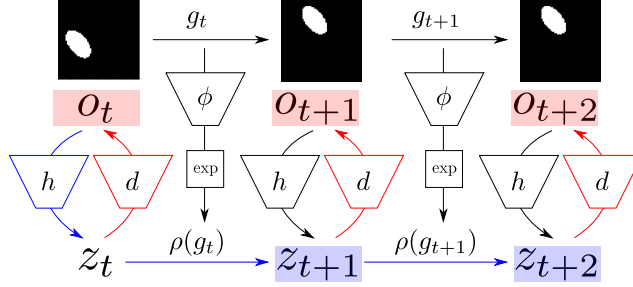


Figure 2: The Homomorphism Autoencoder, consisting of an encoder h , a decoder d and a group representation $\rho = \exp \circ \phi$, relies on 2-step latent prediction to jointly learn the group representation ρ and the observation representation h . Blue highlighted nodes correspond to contributions to the latent prediction loss, while red highlighted nodes correspond to contributions to the reconstruction loss. The blue computation path indicates how future latents z_{t+1}, z_{t+2} are predicted from the encoding of the initial observation z_t through successively applying the group representation.

encoding vectors of observations $z_i = h(o_i)$ to predict the encoding of future images. The latent prediction is evaluated on both the latent space through the latent prediction loss and on the image space through the reconstruction loss.

$$\mathcal{L} = \mathcal{L}_{rec} + \gamma * \mathcal{L}_{pred}$$

The losses are separately detailed in the section 3.3.

3.3 The HAE Learns Symmetry-Based Representations

Previous attempts to design symmetry-based disentangled linear representations have put a lot of emphasis on the disentanglement property. However, it remains unclear how to learn a symmetry-based linear representation (ρ, h) that verifies properties 1 and 2 in section 2.1, without enforcing strong assumptions on ρ [Caselles-Dupré et al., 2019] or on the actions the agent can perform [Caselles-Dupré et al., 2019, Quessard et al., 2020].

In this section, we provide theoretical insights on learning symmetry-based representations and how the two-step HAE architecture achieves that with minimal assumptions.

We define the losses used throughout.

The latent prediction loss compares the evolution of stimuli encodings predicted by using the group representation action (blue computation path in Figure 2) against the encodings of the corresponding observations.

$$\mathcal{L}_{pred}^N(\rho, h) = \sum_t \sum_{j=1}^N \|h(o_{t+j}) - \prod_{i=0}^{j-1} \rho(g_{t+i})h(o_t)\|_2^2$$

The reconstruction loss compares the reconstructions of the stimuli obtained from decoding the predicted evolution of encodings (blue computation path plus the red decoding arrow in Figure 2) against the actual stimuli. The reconstruction loss also evaluates the reconstruction of the initial observation like a standard autoencoder.

$$\mathcal{L}_{rec}^N(\rho, h, d) = \sum_t \sum_{j=0}^N \|o_{t+j} - d(\prod_{i=0}^{j-1} \rho(g_{t+i})h(o_t))\|_2^2$$

where by convention the product for $j = 0$ denotes simply $h(o_t)$, such that the sum of all norm terms corresponding to $j = 0$ form a 0-step reconstruction loss.

The 1-step latent prediction loss is simply enforcing the commutative diagram in Figure 1. With the assumption that the group G is a compact Lie Group, it admits a *faithful* group representation ρ^* that we can assume is the one acting on the world states W . If we assume ρ^* is given on Z , then minimizing $\mathcal{L}_{pred}^1(\rho^*, h)$ is enough to learn a symmetry-based representation.

Proposition 1. Assume we observed the action of the group G on each point of the observation space. Assume h minimizes $\mathcal{L}_{pred}^1(\rho^*, h)$ then h is a symmetry-based representation, meaning $h \circ b$ is equivariant.

However, when ρ^* is not known and a group representation ρ of G needs to be learned over a space of arbitrary mappings, minimizing $\mathcal{L}_{pred}^1(\rho, h)$ can lead to the trivial representation.

Proposition 2. The trivial group representation $\rho = I$ (that always maps to the identity matrix) combined with a constant h is a zero of the prediction loss $\mathcal{L}_{pred}^1(\rho, h)$.

The reconstruction loss of the initial observation helps avoid the representation collapse into a trivial solution by ensuring h is not constant for a given fixed group representation ρ^0 . Although we found using $\mathcal{L}_{rec}^2(\rho, h, d)$ works better than $\mathcal{L}_{rec}^0(\rho, h, d)$ when jointly learning (ρ, h) .

Proposition 3. Assume the data samples at least once all points of the observation space. If h minimizes $\mathcal{L}_{rec}^N(\rho^0, h, d)$ then h is injective.

Next we present our main result stating that the HAE through enforcing the 2-step latent prediction loss and the observations reconstruction (enforcing h is injective) learns a symmetry-based representation.

Proposition 4. Assume (ρ, h) minimizes $\mathcal{L}_{pred}^2(\rho, h)$ and h is injective, then ρ is a non-trivial group representation and (ρ, h) is a symmetry-based representation.

3.4 Disentanglement

Previous works [Caselles-Dupré et al., 2019, Quessard et al., 2020, Painter et al., 2020] assume prior knowledge of the group structure by observing elementary "sparse" actions, that are taken along the subgroups of the group decomposition ("UP", "Down", "LEFT" and "RIGHT") but not in their composition.

In our approach, the HAE learns a group representation without restricting the actions to be observed from the subgroups. Actions can be sampled randomly in a neighbourhood of the identity.

As expressed in section 2.1 the disentanglement condition for a linear action on Z defined through its group representation ρ , is a decomposition of both the representation space $Z = \bigoplus_1^n Z_i$ and the group representation $\rho = \bigoplus_{i=1}^n \rho_i$. Where the subgroup representations ρ_i are representations of the subgroups G_i on the subspaces Z_i .

Following that the group G is decomposed in the true latent's parametrization, the observed group representation is disentangled with regard to the group decomposition if in matrix form, the group representation of any group element $g = \varphi(\tilde{g})$ is a block-diagonal matrix of the subgroups representations:

$$\rho(g = \varphi(\tilde{g}^1, \dots, \tilde{g}^n)) = \begin{pmatrix} \rho_1(\tilde{g}^1) & 0 & \dots & 0 \\ 0 & \rho_2(\tilde{g}^2) & \ddots & \vdots \\ \vdots & \ddots & \ddots & 0 \\ 0 & \dots & 0 & \rho_n(\tilde{g}^n) \end{pmatrix} \quad (2)$$

We can therefore constrain our trainable group representation in the space of matrices of the block diagonal form given in equation 2. This requires prior knowledge of:

- The number of groups in the decomposition.
- The dimension of each subgroup representation $dim(Z_i)$.

We start by assuming knowledge of this information, and we leave the investigation of how to search for the best decomposition for future work. However, we do not assume prior knowledge of the decomposition. Meaning that given an observed transition g , we do not have access to the decomposition $\varphi^{-1}(g) = \tilde{g} = (\tilde{g}^1, \dots, \tilde{g}^n)$ along the group decomposition $G = G_1 \times \dots \times G_n$.

Which means we are learning representations of the form given in equation 3.

$$\rho(g) = \begin{pmatrix} \rho_1(g) & 0 & \dots & 0 \\ 0 & \rho_2(g) & \ddots & \vdots \\ \vdots & \ddots & \ddots & 0 \\ 0 & \dots & 0 & \rho_n(g) \end{pmatrix} \quad (3)$$

While we do not prove that this block diagonal constraint leads to disentanglement, we show through experiments that HAE learns a symmetry-based representation (ρ, h) that is disentangled with regard to the true factors and takes the form in equation 2.

4 Experiments¹

4.1 Learning a 2D-Torus Representation Manifold

We consider a subset of the dSprites dataset [Matthey et al., 2017] where a fixed scale and orientation ellipse is acted on by the group of 2D cyclic translations $G = C_x \times C_y$. The corresponding transition dataset contains tuples $(o_1, g_1, o_2, \dots, g_{n-1}, o_n)$, where the observations o_i are 64×64 pixels and the transitions are given by $g_i = \varphi_{\pi/4}(\tilde{g}_i)$ where $\tilde{g}_i = (\tilde{g}_i^x, \tilde{g}_i^y)$ parametrizes the displacement along x and y , and $\varphi_{\pi/4}$ is the rotation of the 2D plane by 45 deg. We train the 2-step HAE described in section 3.2 with a 4D latent space and with the group morphism $\rho = \exp \circ \phi$ where ϕ maps to a 2-blocks diagonal matrix each of dimension 2×2 . Architecture and hyperparameters for training are specified in the Appendix C.2.

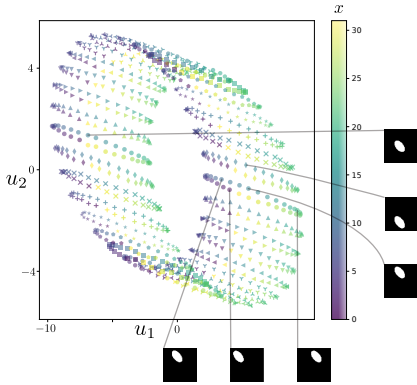


Figure 3: Random 2D projection of the 4D HAE latent encodings of the translated ellipse dataset. Color indicates y position of the ellipse, while markers indicate x position. The visualization is further explained in the Appendix C.2.2 and an alternative visualization is provided in Appendix C.2.4.

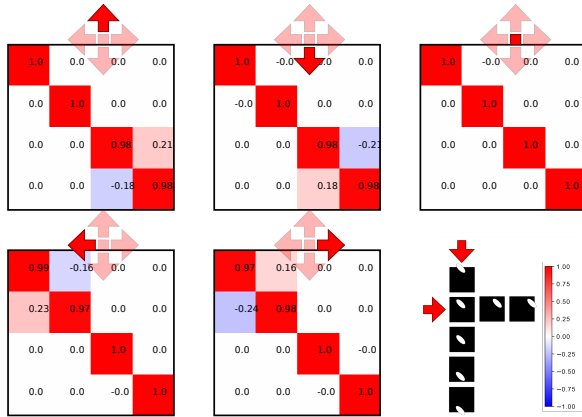


Figure 4: Evaluation of the learned and disentangled group representation ρ for the identity element (upper right) and generative transitions (middle and left) yields block rotation matrices.

Learned data representation We visualize the learned 4-dimensional latent encodings of the whole dataset through 2-dimensional random matrix projections (See Appendix C.2.2), and selected few matrices showing the most discernible projections (Figure 3). The learned manifold corresponds to the expected latent space topology $S^1 \times S^1$.

Learned Group Representation ρ We then evaluate the learned matrices for the identity $id = (0, 0)$, the generating elements of each subgroup $\tilde{1}_x = (1, 0)$, $\tilde{1}_y = (0, 1)$ and their inverses $-\tilde{1}_x = (-1, 0)$, $-\tilde{1}_y = (0, -1)$, Figure 4. Note that the corresponding observed actions g presented to the group representation ρ are in the same order: $(0, 0)$, $\frac{\sqrt{2}}{2}(1, 1)$, $\frac{\sqrt{2}}{2}(-1, 1)$, $\frac{\sqrt{2}}{2}(-1, -1)$, $\frac{\sqrt{2}}{2}(1, -1)$.

¹The code is made available at <https://github.com/hamzakeurti/homomorphismvae>

For the actions in Figure 4 the matrices obtained show that $\rho(0) = I_4$ and that representations for elements belonging to subgroups of the decomposition $G = C_x \times C_y$ follow the disentangled group representation predicted in subsection 3.4 where actions on the same subgroup have representations that act on the same subspace while fixing the other subspace. In addition, the blocks correspond to 2D rotation matrices which are of the form:

$$R(\theta) = \begin{pmatrix} \cos(\theta) & -\sin(\theta) \\ \sin(\theta) & \cos(\theta) \end{pmatrix}$$

The angle of rotation of an elementary step corresponds to the number of equally spaced true latent values for each subgroup: $2\pi/32$, with $\cos(2\pi/32) \approx 0.981$ and $\sin(2\pi/32) \approx 0.195$. Additional information on this setup is available in the Appendix C.2.

4.2 Rollout Prediction

One important application of learning structured representation is to predict how the observations would change given sequences of actions. To test this we compare HAE to two other approaches that model the dynamics in the latent space: (1) *Unstructured*: $z_{t+1} = h(z_t, g_t)$, where h is a learnable function, it jointly encodes the current encoding state z_t and the performed action g_t to predict the next encoding z_{t+1} . This approach does not leverage the structure imposed by the actions g on the encodings z , and learns instead a combinatorial solution to the prediction problem. Similar approaches have been widely adapted in recent model-based deep RL methods [Ha and Schmidhuber, 2018, Schrittwieser et al., 2020]. (2) *Rotations*: $z_{t+1} = R_g z_t$, where $R_g = \prod_{i,j} G(i, j, \theta_{i,j,g})$ and $G(i, j, \theta_{i,j,g})$ are the Givens rotation matrices. The model learns the 2D rotation angles $\theta_{i,j,g}$. This approach was proposed by Quessard et al. [2020] and was shown to be capable of learning symmetry-based representations when the actions are sampled along the true latents.

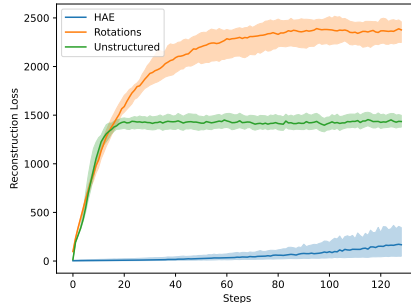


Figure 5: Step-wise reconstruction loss on the test dataset. Lines and shadings represent median and interquartile range over 50 random seeds.

We evaluate the methods in an offline setting, where we train each method on a given set of 2-step trajectories and test their generalization ability on a hold-out set of 128-step trajectories. See Appendix C.3 for details on the setup. Figure 5 shows the reconstruction loss for each method on the test trajectories. Our result suggests that when the actions sampled are not sparse (i.e., each action may involve changes in multiple generating factors), the Rotations method may perform worse than the Unstructured method while HAE can outperform them significantly. In the following section we show how our approach can also disentangle non-acted on properties as an "identity" component of the representation.

4.3 Unsupervised Identity Separation from Intervention

We consider the subset of the dSprites dataset consisting of three shapes (heart, square and ellipse) acted on by the previous group of 2D cyclic translations $G = C_x \times C_y$. The action of the group is not *transitive*, as it describes a separate *orbit* for each shape (see appendix A). Indeed, no intervention changes the shape. In this experiment, we augment the representation space by one dimension to account for the shape property, and the group representation is fixed to act trivially on it.

We learn 5-dimensional encodings of the observations $2 \times 2D$ subspaces acted on by the subrepresentations of the group G and 1 representation unit trivially acted on.

Our results in Figure 6 show that the model not only learns the representation of the cyclic translation group action shared among shapes, but also learns to separate the representation of observations by shape along the last G -invariant representation unit, giving rise to three identical manifolds. This is reminiscent of the two-streams hypothesis of visual processing [Goodale and Milner, 1992], the "What" pathway processes information related to object identity, while the "Where" pathway processes information related to the object pose, or the required motor action for manipulation.

A more thorough description and analysis of the experiment can be found in Appendix C.4.

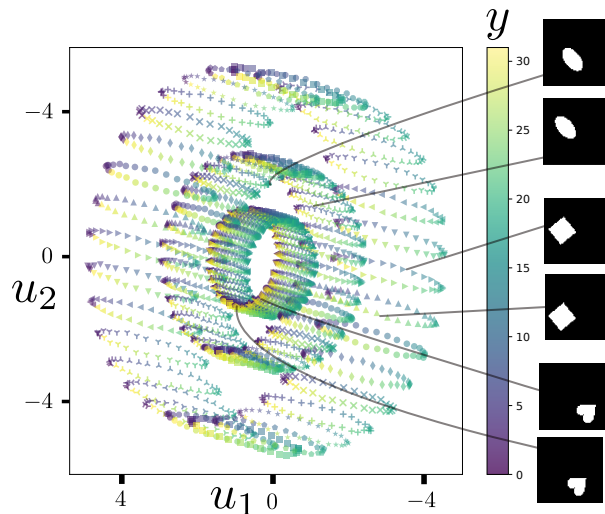


Figure 6: $5D$ representation space of a trained homomorphism autoencoder with two $2D$ group subrepresentations and a $1D$ representation space acted on trivially. The representation vectors for the whole dataset are projected to $2D$ via Random Projection. Colors indicate y position, markers indicate x position and each torus corresponds to a separate shape. The visualization is further explained in the Appendices C.2.2 and C.4 and an alternative visualization is provided in Appendix C.2.4 for a different experiment.

5 Discussion

We provide theoretical and experimental justification that the HAE allows an agent to extract geometric structure of its external world while learning a similarly structured, low dimensional internal manifold. In contrast to earlier works, our only prior assumption is the number of subgroups in the group decomposition, as well as the dimensionality to represent each. When using a set of cyclic actions, we find that the HAE maps the geometric action structure into the agent’s latent space, in the sense that disentangled geometric latent variables representing the motion factors as well as non-geometric variables representing different objects or shapes emerge. In particular, the emergence of invariant object representations provides a new angle for those seeking to learn rich and behavior-relevant representations of objects without the need for labels. Finally, it is interesting to note that similar cyclic embeddings have been reported in neuroscience, for example, in the hippocampus of mice where circular embeddings encode the animals’ head-direction [Chaudhuri et al., 2019]. In fact, our cyclic shape translation task restricted to a single dimension could be viewed as an agent horizontally rotating its head while observing its environment. One limitation of our theoretical analysis is the deterministic nature of our model, the intrinsically non-linear nature of the problem would make the theoretical analysis more challenging in the stochastic setting. On the experimental side, we solely assessed the extraction and internal representation of geometric action structure, we leave it to future work to test if the same principled HAE approach generalizes to learn other, non-cyclic, facets of the structure of the external world.

Acknowledgments and Disclosure of Funding

Hamza Keurti is grateful to CLS for generous funding support. The authors thank the International Max Planck Research School for Intelligent Systems (IMPRS-IS) for supporting Hsiao-Ru Pan. Further this work was supported by the Swiss National Science Foundation (B.F.G. CRSII5-173721 and 315230_189251), ETH project funding (B.F.G. ETH-20 19-01), the Human Frontiers Science Program (RGY0072/2019).

References

- Yoshua Bengio, Aaron Courville, and Pascal Vincent. Representation Learning : A Review and New Perspectives. (1993):1–30, 2012.
- Hugo Caselles-Dupré, Michael Garcia-Ortiz, and David Filliat. Symmetry-based disentangled representation learning requires interaction with environments. In *Advances in Neural Information Processing Systems*, volume 32, 2019.
- Andrea Censi and Richard M. Murray. Learning diffeomorphism models of robotic sensorimotor cascades. *Proceedings - IEEE International Conference on Robotics and Automation*, pages 3657–3664, 2012. ISSN 10504729. doi: 10.1109/ICRA.2012.6225318.
- Rishidev Chaudhuri, Berk Gerçek, Biraj Pandey, Adrien Peyrache, and Ila Fiete. The intrinsic attractor manifold and population dynamics of a canonical cognitive circuit across waking and sleep. *Nature Neuroscience*, 22, 2019.
- Taco S Cohen and Max Welling. Steerable CNNs. *CoRR*, abs/1612.0, 2016. URL <http://arxiv.org/abs/1612.08498>.
- S. M. Ali Eslami, Danilo Jimenez Rezende, Frederic Besse, Fabio Viola, Ari S. Morcos, Marta Garnelo, Avraham Ruderman, Andrei A. Rusu, Ivo Danihelka, Karol Gregor, David P. Reichert, Lars Buesing, Theophane Weber, Oriol Vinyals, Dan Rosenbaum, Neil Rabinowitz, Helen King, Chloe Hillier, Matt Botvinick, Daan Wierstra, Koray Kavukcuoglu, and Demis Hassabis. Neural scene representation and rendering. *Science*, 360:1204–1210, 2018. ISSN 10959203. doi: 10.1126/science.aar6170.
- Melvyn A. Goodale and A. David Milner. Separate visual pathways for perception and action, 1992. ISSN 01662236.
- Luigi Gresele, Julius von Kügelgen, Vincent Stimper, Bernhard Schölkopf, and Michel Besserve. Independent mechanism analysis, a new concept? *arXiv:2106.05200 [cs, stat]*, June 2021. URL <http://arxiv.org/abs/2106.05200>. arXiv: 2106.05200.
- David Ha and Jürgen Schmidhuber. World models. *arXiv preprint arXiv:1803.10122*, 2018.
- Irina Higgins, David Amos, David Pfau, Sebastien Racaniere, Loic Matthey, Danilo Rezende, and Alexander Lerchner Deepmind. Towards a Definition of Disentangled Representations. *arxiv*, dec 2018. doi: 10.48550/arxiv.1812.02230. URL <https://arxiv.org/abs/1812.02230v1>.
- Aapo Hyvarinen and Hiroshi Morioka. Unsupervised Feature Extraction by Time-Contrastive Learning and Nonlinear ICA. *arXiv:1605.06336 [cs, stat]*, May 2016. URL <http://arxiv.org/abs/1605.06336>. arXiv: 1605.06336.
- Georg Keller, Tobias Bonhoeffer, and Marc Hübener. Sensorimotor mismatch signals in primary visual cortex of the behaving mouse. *Neuron*, 74, 2012.
- Ilyes Khemakhem, Diederik Kingma, Ricardo Monti, and Aapo Hyvarinen. Variational Autoencoders and Nonlinear ICA: A Unifying Framework. In *International Conference on Artificial Intelligence and Statistics*, pages 2207–2217. PMLR, June 2020. URL <http://proceedings.mlr.press/v108/khemakhem20a.html>. ISSN: 2640-3498.
- Tejas D Kulkarni, William F Whitney, Pushmeet Kohli, and Josh Tenenbaum. Deep convolutional inverse graphics network. *Advances in neural information processing systems*, 28, 2015.
- Francesco Locatello, Stefan Bauer, Mario Lucie, Gunnar Rätsch, Sylvain Gelly, Bernhard Schölkopf, and Olivier Bachem. Challenging common assumptions in the unsupervised learning of disentangled representations. *36th International Conference on Machine Learning, ICML 2019*, 2019-June: 7247–7283, 2019.
- Loic Matthey, Irina Higgins, Demis Hassabis, and Alexander Lerchner. dsprites: Disentanglement testing sprites dataset. <https://github.com/deepmind/dsprites-dataset/>, 2017.
- Matthew Painter, Jonathon Hare, and Adam Prügel-Bennett. Linear disentangled representations and unsupervised action estimation. *Advances in Neural Information Processing Systems*, 33, 2020.

- Adam Paszke, Sam Gross, Francisco Massa, Adam Lerer, James Bradbury, Gregory Chanan, Trevor Killeen, Zeming Lin, Natalia Gimelshein, Luca Antiga, Alban Desmaison, Andreas Kopf, Edward Yang, Zachary DeVito, Martin Raison, Alykhan Tejani, Sasank Chilamkurthy, Benoit Steiner, Lu Fang, Junjie Bai, and Soumith Chintala. Pytorch: An imperative style, high-performance deep learning library. In H. Wallach, H. Larochelle, A. Beygelzimer, F. d'Alché-Buc, E. Fox, and R. Garnett, editors, *Advances in Neural Information Processing Systems 32*, pages 8024–8035. Curran Associates, Inc., 2019. URL <http://papers.neurips.cc/paper/9015-pytorch-an-imperative-style-high-performance-deep-learning-library.pdf>.
- Jean Piaget. Part I: Cognitive development in children: Piaget development and learning. *Journal of Research in Science Teaching*, 2(3):176–186, 1964. ISSN 10982736. doi: 10.1002/tea.3660020306.
- Robin Quessard, Thomas D. Barrett, and William R. Clements. Learning disentangled representations and group structure of dynamical environments. In *Advances in Neural Information Processing Systems*, volume 2020-December, 2020.
- B. Schölkopf, F. Locatello, S. Bauer, N. R. Ke, N. Kalchbrenner, A. Goyal, and Y. Bengio. Toward causal representation learning. *Proceedings of the IEEE*, 109(5):612–634, 2021.
- Julian Schrittwieser, Ioannis Antonoglou, Thomas Hubert, Karen Simonyan, Laurent Sifre, Simon Schmitt, Arthur Guez, Edward Lockhart, Demis Hassabis, Thore Graepel, et al. Mastering atari, go, chess and shogi by planning with a learned model. *Nature*, 588(7839):604–609, 2020.
- Sumedh A Sontakke, Arash Mehrjou, Laurent Itti, and Bernhard Schölkopf. Causal curiosity: RL agents discovering self-supervised experiments for causal representation learning. In *International Conference on Machine Learning*, pages 9848–9858. PMLR, 2021.
- R. S. Sutton and A. G. Barto. *Reinforcement Learning: An Introduction*. MIT Press, Cambridge, MA, 2nd edition, 2015.
- Valentin Thomas, Jules Pondard, Emmanuel Bengio, Marc Sarfati, Philippe Beaudoin, Marie-Jean Meurs, Joelle Pineau, Doina Precup, and Yoshua Bengio. Independently controllable factors. 2017. doi: 10.48550/arxiv.1708.01289. URL <https://arxiv.org/abs/1708.01289v2>.
- Julius von Kügelgen, Yash Sharma, Luigi Gresele, Wieland Brendel, Bernhard Schölkopf, Michel Besserve, and Francesco Locatello. Self-Supervised Learning with Data Augmentations Provably Isolates Content from Style. *arXiv:2106.04619 [cs, stat]*, June 2021.

A Background on group theory

In this section, we provide an overview of group theory concepts exploited in this work.

Definition A.1 (Group). *A set G is a group if it is equipped with a binary operation $\cdot : G \times G \rightarrow G$ and if the group axioms are satisfied*

1. *Associativity: $\forall a, b, c \in G, (a \cdot b) \cdot c = a \cdot (b \cdot c)$*
2. *Identity: There exists $e \in G$ such that $\forall a \in G, a \cdot e = e \cdot a = a$.*
3. *Inverse: $\forall a \in G, there exists $b \in G$ such that $a \cdot b = b \cdot a = e$. This inverse is denoted a^{-1} .$*

We are often interested in sets of transformations, which respect a group structure, but are applied to objects that are not necessarily group elements. This can be studied through group actions, which describe how groups *act* on other mathematical entities.

Definition A.2 (Group Action). *Given a group G and a set X , a group action is a function $\cdot_X : G \times X \rightarrow X$ such that the following conditions are satisfied.*

1. *Identity: If $e \in G$ is the identity element, then $e \cdot_X x = x, \forall x \in X$.*
2. *Compatibility: $\forall g, h \in G$ and $\forall x \in X, g \cdot_X (h \cdot_X x) = ((g \cdot h) \cdot_X x)$*

The group action $\cdot_X : G \times X \rightarrow X$ induces a group homomorphism $\rho_{\cdot_X} : G \rightarrow Sym(X)$. (where $Sym(X)$ is the group of all invertible transformations of X) through:

$$\forall (g, x) \in G \times X, \quad g \cdot_X x = \rho_{\cdot_X}(g)(x)$$

The group homomorphism property of ρ_{\cdot_X} comes from the group action axioms of \cdot_X :

$$\begin{aligned} \rho_{\cdot_X}(id)(x) &= id \cdot_X x = x \quad (\text{identity}) \\ &= id_X(x) \end{aligned}$$

So $\rho_{\cdot_X}(id) = id_X$. and

$$\begin{aligned} \rho_{\cdot_X}(g_1 \cdot g_2)(x) &= (g_1 \cdot g_2) \cdot_X x = g_1 \cdot_X (g_2 \cdot_X x) \quad (\text{compatibility}) \\ &= \rho_{\cdot_X}(g_1) \circ \rho_{\cdot_X}(g_2)(x) \end{aligned}$$

Equality over all of X leads to equality of the functions: $\rho_{\cdot_X}(g_1 \cdot g_2) = \rho_{\cdot_X}(g_1) \circ \rho_{\cdot_X}(g_2)$.

In what follows, we are interested in *linear group actions* in which case the acted on space is a vector space V and the induced homomorphism ρ maps G to the group $GL(V)$ of invertible linear transformations of V . This mapping is called a group representation. Actions of this type have been studied extensively in representation theory.

Definition A.3 (Group Representation). *Let G be a group and V a vector space. A representation is a function $\rho : G \rightarrow GL(V)$ such that $\forall g, h \in G, one has $\rho(g)\rho(h) = \rho(g \cdot h)$.$*

Note that such definition is not restricted to finite dimensional vector spaces, however we will limit our study to this case, such that representations are appropriately described by mappings from G to a space of square matrices.

Definition A.4 (Lie Group). *A Lie Group G is a nonempty set satisfying the following conditions:*

- *G is a group.*
- *G is a smooth manifold.*
- *The group operation $\cdot : G \times G \rightarrow G$ and the inverse map $\cdot^{-1} : G \rightarrow G$ are smooth.*

We limit ourselves to the study of linear Lie Groups, Lie groups that are matrix groups. The tangent space to a Lie Group at the identity forms a Lie Algebra. A Lie Algebra \mathfrak{g} is a vector space equipped with a bilinear map $[\cdot, \cdot] : \mathfrak{g} \times \mathfrak{g} \rightarrow \mathfrak{g}$ called the Lie Bracket. We will not introduce the Lie Bracket as we do not make use of it. The Lie Algebra somehow describes most of everything happening in its Lie Group. This connection is established through the exponential map.

Definition A.5 (Exponential Map). *The exponential map $\exp : \mathfrak{g} \rightarrow G$ is defined for matrix Lie Groups by the series:*

$$e^A = \sum_{k=0}^{\infty} \frac{1}{k!} A^k. \quad \forall A \in \mathfrak{g}$$

The exponential map is not always surjective. However if we only consider groups that are connected and compact, the exponential is surjective, which justifies our parametrization of the group representation through:

$$\rho : G \xrightarrow{\phi} \mathfrak{g} = M_n(\mathbb{R}) \xrightarrow{\exp} GL_n(\mathbb{R})$$

Where ϕ is a trainable arbitrary mapping.

Group action types The effect of a group action on a base space X varies according to the properties of the homomorphism defined by the group action

$$\begin{aligned} \tau : G &\rightarrow \text{Sym}(X) \\ g &\mapsto g \cdot_X \square \end{aligned}$$

We introduce two types of actions:

Definition A.6 (Transitive Group Action). *The action of G on X is transitive if X forms a single orbit.*

in other words, $\forall x, y \in X, \exists g \in G; g \cdot x = y$.

Definition A.7 (Faithful Group Action). *The action of G on X is faithful if the homomorphism $G \rightarrow \text{Sym}(X)$ corresponding to the action is bijective (an isomorphism).*

In that case, $\forall g_1 \neq g_2 \in G, \exists x \in X; g_1 \cdot x \neq g_2 \cdot x$.

We also define the *orbits* by a group action:

Definition A.8 (Orbit by a Group Action). *The orbit of an element $x \in X$ by the action \cdot_X of a group G is the set*

$$G \cdot_X x = \{g \cdot_X x : g \in G\}$$

When the action of G is transitive on X , then X is the single orbit by the action of G :

$$\forall x \in X, G \cdot_X x = X$$

Such is the case for our experiments using a single shape. We also explore the case where the action is not transitive in the multi shape experiment visualized in Figure 6.

B Theoretical results

First we prove the main theoretical result of the paper, then proceed to prove the other propositions.

Proposition 4. *Assume (ρ, h) minimizes $\mathcal{L}_{pred}^2(\rho, h)$ and h is injective, then ρ is a non-trivial group representation and (ρ, h) is a symmetry-based representation.*

Proof. Given that the group G is supposed compact, it admits a group representation by the *Peter-Weyl theorem*. We can therefore assume that the true state space W is acted on linearly by G through its representation ρ^* . As such the inverse of the generating process b^{-1} and ρ^* verify $\mathcal{L}_{pred}^2(\rho^*, b^{-1}) = 0$.

Assume h is injective, guaranteed by a minimization of the 0-step reconstruction loss.

Assume (ρ, h) minimizes $\mathcal{L}_{pred}^2(\rho, h)$ therefore $\mathcal{L}_{pred}^2(\rho, h) = 0$.

Then for all observed 2-step transitions $(o_t, g_t, o_{t+1}, g_{t+1}, o_{t+2})$ — note that observed transitions (o_t, g_t, o_{t+1}) correspond to an action on the true world states $w_{t+1} = g_t \cdot_W w_t$ — (ρ, h) verifies:

$$\rho(g_t)h(o_t) = h(o_{t+1})$$

and

$$\rho(g_{t+1})\rho(g_t)h(o_t) = h(o_{t+2})$$

Let us prove ρ is a group representation, meaning it verifies $\rho(g_2g_1) = \rho(g_2)\rho(g_1), \forall g_1, g_2 \in G$.

Let $g_1, g_2, g_3 \in G$ such that $g_3 = g_2g_1$.

Let w_1, w_2, w_3 which verify $w_2 = g_1 \cdot_W w_1, w_3 = g_2 \cdot_W w_2, w_3 = g_3 \cdot_W w_1$. Therefore, the associated transitions $(o_1, g_1, o_2), (o_2, g_2, o_3)$ and (o_1, g_3, o_3) can be observed.

$$\begin{array}{ccccc} o_1 & \xrightarrow{g_1} & o_2 & \xrightarrow{g_2} & o_3 \\ & & & \searrow & \nearrow \\ & & & g_2g_1 & \end{array}$$

Assume, we observe the 2-step transitions $(o_t, g_t, o_{t+1}, g_{t+1}, o_{t+2})$ and $(o_{t'}, g_{t'}, o_{t'+1}, g_{t'+1}, o_{t'+2})$ such that:

$$\begin{cases} o_t = o_{t'} = o_1 \\ o_{t+1} = o_2 \\ o_{t+2} = o_{t'+1} = o_3 \end{cases}$$

and

$$\begin{cases} g_t = g_1 \\ g_{t+1} = g_2 \\ g_{t'+1} = g_3 = g_2g_1 \end{cases}$$

$\mathcal{L}_{pred}^2 = 0$ gives for the transition at t : $\rho(g_{t+1})\rho(g_t)h(o_t) = h(o_{t+2})$ therefore $\rho(g_2)\rho(g_1)h(o_1) = h(o_3)$.

And for the transition at t' : $\rho(g_{t'})h(o_{t'}) = h(o_{t'+1})$ therefore $\rho(g_3)h(o_1) = h(o_3)$

Therefore we have $\rho(g_2)\rho(g_1)h(o_1) = \rho(g_3)h(o_1)$ or $\rho(g_2)\rho(g_1)h(o_1) = \rho(g_2g_1)h(o_1)$

With this equality verified over the set O_{tr} of first observations o_1 in the training set — meaning we observe two successions of the action of group elements (g_1, g_2) and g_3 for different values of the starting observation o_1 — by assuming $h(O) \subseteq \text{span}(h(O_{tr}))$, we get that $\rho(g_2)\rho(g_1) = \rho(g_2g_1)$ over $h(O)$ (equality of linear mappings over vectors that span a vector subspace).

Therefore the subrepresentation of ρ over $\text{span}(h(O))$ is a group representation of G .

The injectivity assumption ensure $h(O)$ does not collapse to a single element.

Let us show h is a symmetry based representation.

We have for every observed transition (o_t, g_t, o_{t+1}) :

$$h(o_{t+1}) = \rho(g_t)h(o_t)$$

by the generative model assumptions

$$o_{t+1} = b(w_{t+1}) = b(g_t \cdot_W w_t)$$

Also $o_t = b(w_t)$, finally

$$h \circ b(g_t \cdot_W w_t) = \rho(g_t)h \circ b(w_t)$$

□

Proposition 1. Assume we observed the action of the group G on each point of the observation space. Assume h minimizes $\mathcal{L}_{pred}^1(\rho^*, h)$ then h is a symmetry-based representation, meaning $h \circ b$ is equivariant.

Proof. Given that the group G is supposed compact, it admits a group representation by the *Peter-Weyl theorem*. We can therefore assume that the true state space W is acted on linearly by G through its representation ρ^* . As such the inverse of the generating process b^{-1} and ρ^* verify $\mathcal{L}_{pred}^2(\rho^*, b^{-1}) = 0$.

As a consequence, h also achieves zero loss such that

$$\sum_t \sum_{j=1}^N \|h(o_{t+j}) - \prod_{i=0}^{j-1} \rho^*(g_{t+i})h(o_t)\|_2^2$$

such that for all (j, t)

$$h(o_{t+j}) = \prod_{i=0}^{j-1} \rho^*(g_{t+i})h(o_t)$$

In particular for $j = 1$

$$h(o_{t+1}) = \rho^*(g_t)h(o_t)$$

by the generative model assumptions

$$o_{t+1} = b(w_{t+1}) = b(\rho^*(g_t)w_t)$$

Also $o_t = b(w_t)$ such that

$$h \circ b(\rho^*(g_t)w_t) = \rho^*(g_t)h \circ b(w_t)$$

□

Proposition 3. Assume the data samples at least once all points of the observation space. If h minimizes $\mathcal{L}_{rec}^N(\rho^0, h, d)$ then h is injective.

Proof. Assume the encoder h and the decoder d minimize the 0-step reconstruction.

$$\forall o, o' \in O, \text{ such that } o \neq o'.$$

$$d(h(o)) = o \text{ and } d(h(o')) = o'$$

Therefore

$$d(h(o)) \neq d(h(o')).$$

Finally

$$h(o) \neq h(o')$$

Therefore h is injective.

□

Proposition 5. Assume $h = h^*$ disentangled, equivariantly maps observations in O to Z such that there exists a non-trivial disentangled linear action ρ^* of G on Z according to the group decomposition $G = G_1 \times \dots \times G_n$.

Assume ρ of the form in equation 3 minimizes $\mathcal{L}_{pred}^2(\rho, h^*)$ then ρ is a group representation and ρ defines the same action as ρ^* over the subspace spanned by $h^*(O)$.

Proof. We assume the existence of (h^*, ρ^*) such that ρ^* is a disentangled representation of G with regard to the decomposition $G = G_1 \times \dots \times G_n$ and h^* is an equivariant representation with regard to ρ^* .

As such, ρ^* verifies:

$$\rho^* = \rho_1^* \oplus \dots \oplus \rho_n^*$$

such that

$$\forall i, \forall g = (g_1, \dots, g_n) \in G_1 \times \dots \times G_n; \rho_i^*(g) = \rho_i^*(g_i)$$

h^* verifies

$$h^* \circ b(g \cdot_W w_t) = \rho(g)h^* \circ b(w_t)$$

equivalently, in terms of an observed transition (o_t, g, o_{t+1}) :

$$h^*(o_{t+1}) = \rho^*(g)h^*(o_t)$$

We assume h^* is given but not ρ^* . If $\rho = \rho_1 \oplus \dots \oplus \rho_n$ satisfies $\mathcal{L}_{pred}^2(\rho, h^*) = 0$, then for a given $g \in G$:

$$h^*(o_{t+1}) = \rho(g)h^*(o_t)$$

Then:

$$\rho^*(g)h^*(o_t) = \rho(g)h^*(o_t)$$

is verified for all observations $o_t \in O$. Which leads to the equality of the matrices over the subspace spanned by $h(O)$.

Note that for each g , it is enough to observe the transitions (o_t, g, o_{t+1}) such that $o_t \in O_S$ such that $h(O)$ is in the span of $h(O_S)$.

□

Proposition 6. Assume $\rho = \rho^*$ a non-trivial disentangled group representation of G on Z .

Assume h minimizes $\mathcal{L}_{pred}^2(\rho^*, h)$ then h is a symmetry based disentangled representation with regard to the disentangled group representation ρ^* .

Proof. Given that the group G is supposed compact, it admits a group representation by the Peter-Weyl theorem. We can therefore assume that the true state space W is acted on linearly by G through its representation ρ^* . As such the inverse of the generating process b^{-1} and ρ^* verify $\mathcal{L}_{pred}^2(\rho^*, b^{-1}) = 0$.

Assume h minimizes \mathcal{L}_{pred}^2 then it achieves zero loss such that

$$\sum_t \sum_{j=1}^N \|h(o_{t+j}) - \prod_{i=0}^{j-1} \rho^*(g_{t+i})h(o_t)\|_2^2$$

such that for all (j, t)

$$h(o_{t+j}) = \prod_{i=0}^{j-1} \rho^*(g_{t+i})h(o_t)$$

In particular for $j = 1$

$$h(o_{t+1}) = \rho^*(g_t)h(o_t)$$

by the generative model assumptions

$$o_{t+1} = b(w_{t+1}) = b(g_t \cdot_W w_t)$$

Also $o_t = b(w_t)$, finally

$$h \circ b(g_t \cdot_W w_t) = \rho^*(g_t)h \circ b(w_t)$$

□

C Experiments

C.1 Data

We use a subset of the dSprites dataset consisting only of the ellipse at a fixed scale and orientation with varying x and y positions, there are 32 equally spaced positions for each. We consider that the ellipse is acted on by the group $G = G_x \times G_y$ of cyclic translations, where the sprite warps to the opposite extremity when it reaches an extremal position. For each image o_1 we sample group elements $\tilde{g}_1 = (\tilde{g}_x, \tilde{g}_y)$ uniformly from a square around identity spanning the range $\llbracket -10, 10 \rrbracket$. We assume the agent observes $g_1 = \varphi_{45}(\tilde{g}_1) = \frac{\sqrt{2}}{2}(\tilde{g}_x - \tilde{g}_y, \tilde{g}_x + \tilde{g}_y)$. We obtain the first transition (o_1, g_1, o_2) , we do the same for o_2 to get 2-step transitions $(o_1, g_1, o_2, g_2, o_3)$.

C.2 Learning a disentangled representation

C.2.1 Hyperparameters

Model architecture We use a symmetrical architecture for the encoder and decoder, which we summarize in Table 1. The network was trained on the combined loss:

$$\mathcal{L} = \mathcal{L}_{rec}^2(\rho, h, d) + \gamma \mathcal{L}_{pred}^2(\rho, h)$$

Where we use the Binary Cross Entropy loss for the reconstruction term instead of the Mean Squared Error as it is better behaved during training.

Table 1: Network architecture.

Parameter	Value
Conv. Channels	[64, 64, 64, 64]
Kernel Sizes	[6, 4, 4, 4]
Strides	[2, 2, 1, 1]
Linear Layer Size	1024
Activation	ReLU
Latent space	4
γ	400
Group representation dimensions	[2,2]

Training hyperparameters We trained the network using the hyperparameters summarized in Table 2.

Table 2: Training hyperparameters.

Parameter	Value
Optimizer	Adam
Learning rate	0.001
Number of training sequences	10000
Batch size	500
Epochs	101

C.2.2 Visualization

We obtained Figure 3 by projecting the 4D representation vector for each image in the dataset on a random 2D plane through Random Matrix Projection. We chose the projection with the most explainable visualization.

C.2.3 Latent Traversal

We show how learning a mapping to the group algebra can be leveraged to navigate the group and the data manifold. We remind that $\rho = \exp \circ \phi$, where ϕ maps to the algebra \mathfrak{g} of the group G , and \exp is the matrix exponential which gives a connection between the algebra and the lie group.

The mapping $\phi = \phi_1 \oplus \phi_2$ and the group representation $\rho = \rho_1 \oplus \rho_2$ are constrained on the space of block diagonal matrices of the form $M = M_1 \oplus M_2$ each of dimension 2×2 . However since each block is made of elements from a 1D subgroup of $GL_2(\mathbb{R})$: $SO(2)$, its algebra is the 1D subalgebra of $M_2(\mathbb{R})$ of skew-symmetric matrices. We find this subspace by performing a PCA over each of the sets $\{\phi_1(g_t)\}_t$ and $\{\phi_2(g_t)\}_t$ for a batch $\{g_t\}_t$ of observed transitions. The first component for each block E_1 and E_2 corresponds to the only base vector for that subalgebra. We find:

$$E_1 \oplus 0_{2,2} = \begin{bmatrix} -0.04 & -0.65 & 0 & 0 \\ 0.76 & -0.04 & 0 & 0 \\ 0 & 0 & 0 & 0 \\ 0 & 0 & 0 & 0 \end{bmatrix}$$

$$0_{2,2} \oplus E_2 \approx \begin{bmatrix} 0 & 0 & 0 & 0 \\ 0 & 0 & 0 & 0 \\ 0 & 0 & 0.01 & -0.65 \\ 0 & 0 & 0.76 & 0.01 \end{bmatrix}$$

We obtain the figure 7 by linearly traversing the subalgebras through $t(E_1 \oplus 0_{2,2})$ and $t(0_{2,2} \oplus E_2)$ for equally spaced values of $t \in \llbracket 0, 9 \rrbracket$ and passing it to the matrix exponential which yields invertible matrices of the form $R_{1,t} = e^{tE_1} \oplus I_2$ and $R_{2,t} = I_2 \oplus e^{tE_2}$. We encode an arbitrary initial observation to obtain its representation vector z , and traverse the latent space through $R_{i,t}z$. We decode the obtained vectors to obtain the predicted images.

The group algebra offers a smooth parametrization of the group and consequently of the data manifold and enables the prediction of observations evolution in the absence of performed actions. Indeed, in the above example, all transformations can be obtained in the form $\exp(t_1 E_1) \oplus \exp(t_2 E_2)$ for $t_1, t_2 \in \mathbb{R}$.

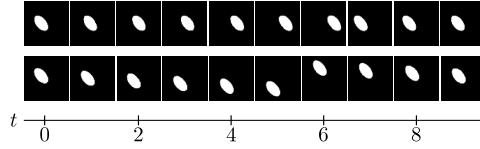


Figure 7: We visualize the linear traversal of the group algebra and its effect on the predicted image reconstruction. The first line corresponds to a traversal $tE_1 \oplus 0_{2,2}$, while the second line corresponds to the traversal $0_{2,2} \oplus tE_2$.

C.2.4 Additional Experiment

We consider a subset of the dataset consisting of all variations of the heart under a fixed scale. As such the heart is acted on by the group $G = G_\theta \times G_x \times G_y = C_{39} \times C_{32} \times C_{32}$. We train a similar model to the one described in the section C.2.1 by changing the latent space to 6 dimensions, the group representation is fixed of the form $\rho = \rho_1 \oplus \rho_2 \oplus \rho_3$ each of dimension 2. We expect a disentangled representation space $Z = Z_1 \oplus Z_2 \oplus Z_3$. For the visualization of the learned representation manifold Figure 8, we visualize each subspace Z_i separately by only varying one generative factor and keeping all else fixed. We also visualized the learned representations for a subset of transitions corresponding to the elementary generative transitions for each subgroup in Figure 9.

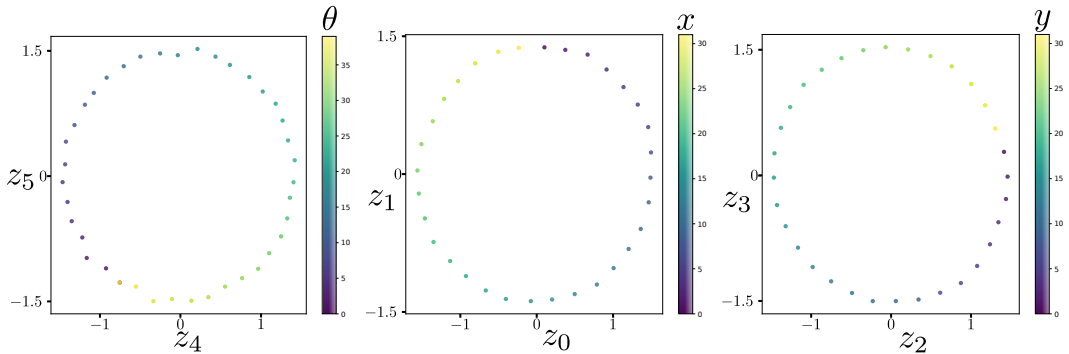


Figure 8: Visualizaion of the 6D embedding vectors for the heart dataset. For each visualized 2D subspace, we only vary the latent represented by the subspace.

C.3 Rollouts prediction

We perform the rollout experiment using the sampling strategy described in Section 3.1 where actions were sampled around the identity uniformly. For simplicity, we reduce the range of the actions from $\llbracket -10, 10 \rrbracket$ to $\llbracket -3, 3 \rrbracket$. Similarly, we only consider x-y translations in this experiment.

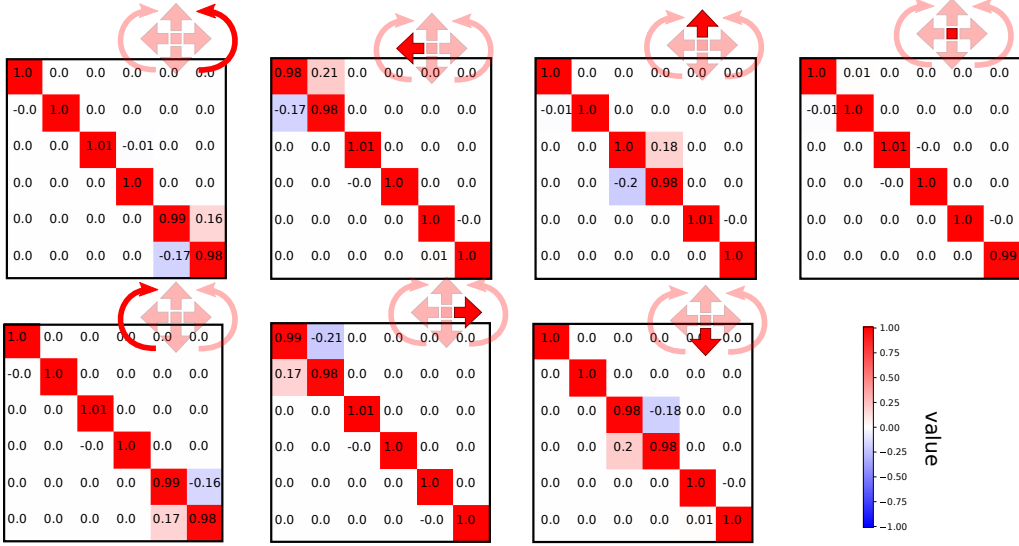


Figure 9: Evaluation of the learned group representation for the identity (upper left) and generative transitions of each subgroup yields disentangled block rotation matrices.

We train each method with a set of pre-generated set of 2-step trajectories and evaluate on a hold-out pre-generated set of 128-step trajectories. For each trajectory, we begin by sampling a random initial state (x,y position) from all possible states.

After that, we sample actions uniformly from the possible actions at each step until the number of steps is satisfied.

For HAE, we map actions to block-diagonal matrices as described in Section 3.2. For the Rotations method [Quessard et al., 2020], we map each action to a matrix $\rho(g)$ through a lookup table for all possible actions. For the Unstructured method, we use a 2 layer MLP of size [128, 128] to model the transition by $z_{t+1} = f_{\theta}(z_t, g_t)$, where we concatenate the latent vector z_t and the one-hot encoding of action a_t .

The reconstruction loss is the same for all three methods, as described in Section 3.3. For HAE, we additionally add the latent prediction loss \mathcal{L}_{pred} as described in Section 3.3. We increase γ to 1600 which we found to be more stable when matrices are directly parameterized instead of mapped from MLPs. For the Rotations method, an additional entanglement loss \mathcal{L}_{ent} is required to encourage each matrix to act on a specific subspace of the latent space, which is equal to

$$\mathcal{L}_{ent} = \sum_g \sum_{(i,j) \neq (\alpha,\beta)} |\theta_{i,j}^g|^2 \quad \text{with} \quad \theta_{\alpha,\beta}^g = \max_{i,j} |\theta_{i,j}^g|.$$

For the Unstructured method, we only use the reconstruction loss and no additional terms.

We also perform another experiment which adapts the setting of multi-step prediction as in Quessard et al. [2020], where agents can perform multiple simple actions (actions only involve changes in a single generating factor) to the object. In our experiment, we allow the agent to control the object in the dSprite dataset with 7 actions. Namely, translation in the x-y axes, rotation in both directions (clockwise, counter-clockwise), and idle. Each action corresponds to an increment/decrement in one of the generating factors of the dataset, except for idle, which does nothing. Additionally, we use the heart shape from the dataset to fully utilize the orientation latent factor. Figure 10 shows that the Rotations method performs better than the Unstructured method in this setting. This is likely because the actions sampling process satisfies the disentanglement assumption described in Quessard et al. [2020]. However, we see that HAE still outperforms both significantly, suggesting that HAE can also learn efficiently under this setting.

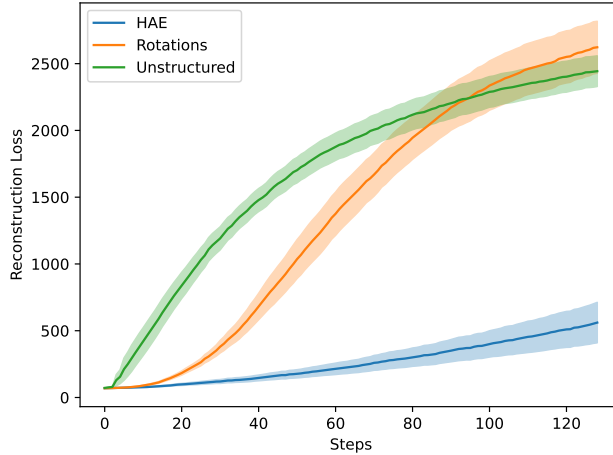


Figure 10: Step-wise reconstruction loss on the test dataset. Lines and shadings represent median and interquartile range over 50 random seeds.

C.4 Multi-objects

We use a similar dataset to the one described in section C.2 except that we use all three shapes: Heart, Ellipse and Square. Because we are considering the action of the same group, observation sequences that start with a given shape have the same shape throughout at different positions. We use a model with a 5D latent, where the last latent is acted on trivially, meaning that the group representation keeps it unchanged. This is equivalent to having a representation of the form $\rho = \rho_x \oplus \rho_y \oplus 1$. We also project the 5D encodings of the dataset on a 2D space through Random Matrix Projection. Note that although the three different tori appear of different sizes, it is only an artifact of the projection while the tori are identical.

C.5 Computational resources

The experiments were performed on an NVIDIA GeForce RTX 3090 and A100 GPUs. The training of our optimal models run for approximately 20 mins.

D Third-Party Software

D.1 Deep Learning Framework

To implement our architecture we used the deep learning framework PyTorch. Paszke et al. [2019]

D.2 Hyperparameter Search

We used the hyperparameter search utility provided in the hypnettorch project <https://github.com/chrhenning/hypnettorch/tree/master/hypnettorch/hpsearch> to perform a random grid search.

D.3 Dataset

In the presented experiments, we used the dSprites dataset Matthey et al. [2017]. The dSprites dataset is an image dataset of white sprites on a black background, varying in shape (heart, ellipse, square), in scale (6 values), in orientation (39 values, cyclic), in x and y position (32 values each). We consider all factors besides shape to be cyclic, in particular for the x and y positions, we "glued" opposite borders of images into a torus. The resolution of the images is 64×64 pixels.

E Societal Impact

This work proposes new findings in basic research. To the best of our knowledge, this work does not have immediate applications with a negative societal impact.